IJCRT.ORG ISSN : 2320-2882

INTERNATIONAL JOURNAL OF CREATIVE RESEARCH THOUGHTS (IJCRT)

An International Open Access, Peer-reviewed, Refereed Journal

Implementation Of Bi-Directional DC-DC Converter For Hybrid Energy Storage Systems

[1]Bhukya Ravi, [2]Dr.P. Satish Kumar

[1]Research Scholar, [2]Professor

[12]Department o Electrical Engineering,

Osmania University, Hyderabad-500007, Telangana, India.

Abstract: Due to the widespread integration of renewable energy sources in DC microgrids, these microgrids are highly vulnerable to fluctuations in power generation, particularly concerning voltage stability. To mitigate these fluctuations, a Hybrid Energy Storage System (HESS) comprising both a battery and a supercapacitor (SC) is employed. The distinct characteristics of batteries and supercapacitors make them an ideal combination for applications in HESS. The HESS is connected to the DC microgrid through a double-input bidirectional converter, offering decoupled control of battery and supercapacitor power, along with facilitating energy exchange between the storage components. This paper introduces a modeling approach for the double-input bidirectional converter and designs a controller for voltage regulation in a DC microgrid. The modified operation of the converter enables the use of the same controller for both HESS charging and discharging operations, creating a unified controller. The designed controller proves effective in rejecting disturbances from both the source and load sides while ensuring the voltage stability of the DC microgrid. The proposed modified operation of the bidirectional converter maintains the State of Charge (SOC) of the low Equivalent Series Resistance (ESR) supercapacitor within the desired range. Simulation results validate the operation of the modified converter and the performance of the designed controller in maintaining voltage stability.

Index Terms - Bi-directional converter, Battery, SC, HESS and PI Controller.

Introduction

Due to the seamless integration with renewable energy sources and the proliferation of DC-compatible loads, DC microgrids are becoming increasingly popular [1], [2]. The high penetration of intermittent renewable energy sources into DC microgrids creates a power mismatch between the generation and load sides, resulting in variations in DC bus voltage. Various Energy Storage Systems (ESS) with diverse characteristics are employed to address this issue, with batteries being the most commonly used ESS. Batteries are preferred for their high energy density, while supercapacitors are favored for their high power density [3], [4]. Intermittent renewable energy sources necessitate an ESS with high energy density, whereas loads with high-pulse requirements demand an ESS with high power density. Consequently, a Hybrid Energy Storage System (HESS) is formed by combining batteries and supercapacitors, meeting the aforementioned requirements of a DC grid [5]-[8]. Furthermore, HESS enhances the stability of power converter-based microgrids, which would otherwise be low due to low rotational inertia [9].

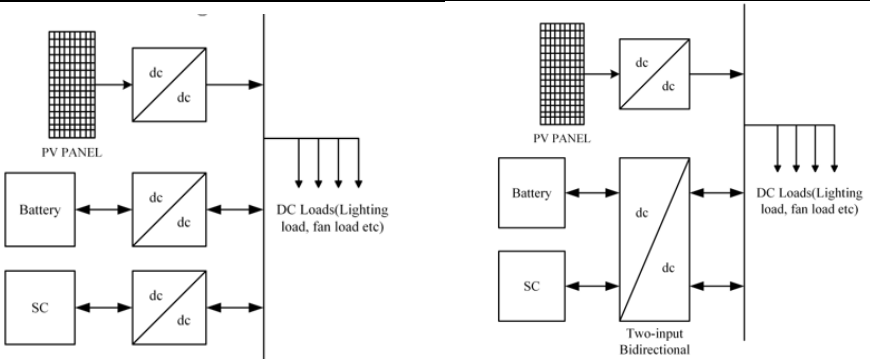

(a) (b)

Figure 1. Various configurations of Hybrid Energy Storage Systems (HESS) involving batteries and supercapacitors interfaced with a DC microgrid are presented. (a) Two distinct bidirectional converter modules are employed. (b) A single double-input bidirectional converter is utilized.

To harness the benefits of both batteries and supercapacitors, various topologies of Hybrid Energy Storage Systems (HESS) were presented in [10]. The most widely utilized configuration of HESS, allowing independent control over both the battery and supercapacitor, is depicted in Figure 1(a). In this active parallel configuration of HESS, there is the capability to transfer energy between the component Energy Storage Systems (ESSs), such as charging the supercapacitor ESS using the battery ESS and vice versa. However, the energy exchange process occurs through the DC microgrid, potentially pushing the grid operating limits beyond the desired range. Alternatively, multiple-input bidirectional converters, as illustrated in Figure 1(b), exhibit superior energy exchange performance between input sources compared to employing multiple single-input bidirectional DC-DC converters in an active parallel configuration.

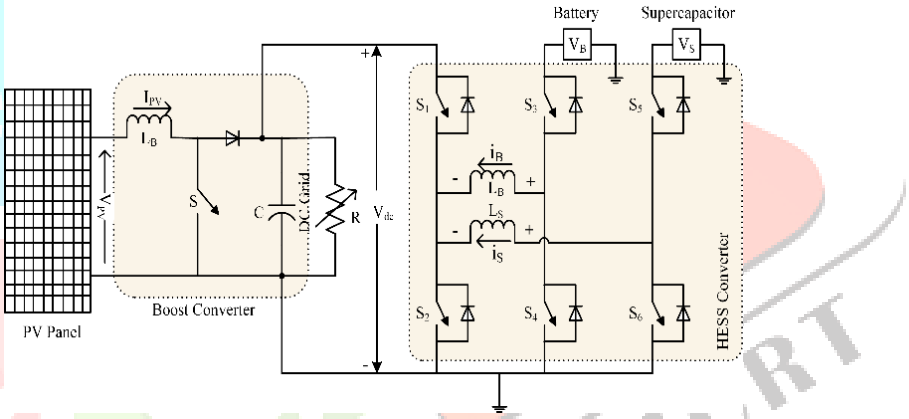

Figure 2. The DC microgrid is energized by a PV source and complemented by a Hybrid Energy Storage System (HESS).

The main contributions of the paper are:

1. A DC microgrid voltage stabilization system is proposed, utilizing a multi-input converter.
2. The chapter includes a detailed controller design and analysis for a Hybrid Energy Storage System (HESS) based on the multi-input bidirectional converter (MIBD).
3. An energy management system (EMS) for the MIBD with HESS is implemented, accommodating various Photovoltaic (PV) and load conditions. The EMS effectively tracks the state of charge (SOC) of the supercapacitor (SC) and facilitates different modes for safe operation.
4. The designed double-input bidirectional converter offers advantages in energy exchange, allowing independent charging of the SC from the battery. Additionally, the converter provides benefits such as efficient power allocation among different Energy Storage Systems (ESSs), rapid control of DC link voltage in response to PV power fluctuations and load disturbances.
5. The proposed modification in the converter's operation enables the use of the same controller for both HESS charging and discharging operations, resulting in a unified controller.

II. TWO INPUT BIDIRECTIONAL DC-DC CONVERTER OPERATION

Figure 2 illustrates the two-input bidirectional converter, and its various operational modes are detailed in [27]. The modified operation of the converter is outlined here, comprising three switch-legs. The battery (VB) and supercapacitor (VS) modules are linked to legs 2 and 3, respectively, while the DC microgrid (VDC) is connected to leg 1. In this converter topology, the battery voltage is chosen to be lower than the DC grid voltage but higher than the supercapacitor voltage. High-frequency inductors LB and LS are interconnected between legs 1, 2, and 1, 3, respectively. The subsequent sections elaborate on different modes of operation.

2.1 HESS Discharging Mode

When there is a disparity between the PV output and the load power, the DC microgrid voltage deviates from its steady-state value. If the load exceeds the PV generation capability or the PV-generated power decreases due to reduced solar irradiation, the DC microgrid voltage decreases. During this period, deficient power needs to be supplied by the HESS. Power flows from the HESS to the DC microgrid in this mode, controlled by the bidirectional converter.

The operation of the converter in this mode can be segmented into three time intervals, as shown in Fig. 2. Switch pairs S_1/S_2, S_3/S_4, and S_5/S_6 always operate complementarily. Switch pairs S_2/S_5 and S_1/S_6 switch together, and their gating pulses are complementary. At time instant t_0, switches S_2, S_3, and S_5 are turned on, increasing inductor currents i_B and i_S linearly with slopes V_B/L_B and V_S/L_S, respectively. At t_1, switch S_3 is turned off to provide a free-wheeling path for current i_B through the body diode of S_4. After the dead time interval for switch pairs S_3/S_4, switch S_4 is turned on. Since the body diode of S_4 is already conducting when the gating signal was given, S_4 turns on with Zero Voltage Switching (ZVS).

At t_2, switches S_2 and S_5 are turned off, causing inductor current i_{L2} to flow through the body diodes of switches S_1 and S_6 with a negative slope of V_{DC}/L_S. Inductor current i_B also flows through the body diode of S1 with a negative slope of V_{DC}/L_B. Switches S_1 and S_6 are gated on after the dead time interval of switch pairs S_2/S_1 and S_5/S_6. Similar to the turn-on of S_4, switches S_1 and S_6 are also turned on with ZVS since the body diodes of the respective switches are already in conduction.

At t_3, switches S_1, S_4, and S_6 are turned off. Consequently, the body diodes of switches S_2, S_3, and S_5 will conduct to maintain the flow of inductor currents. Currents, i_B and i_S, flow with positive slopes of V_B/L_B and V_S/L_S, respectively. After the dead time interval, gating pulses are given to switches S2, S3, and S5, which turn on with ZVS. If d_B is the duty cycle of the gating pulse given to switch S_3, and d_S is the duty cycle of the gating pulse given to switches S_2 and S_5, applying volt-second balance to inductors L_S and L_B gives:

$$V_{DC} = \frac{d_S}{1-d_S}.V_S$$

$$V_{DC} = \frac{d_B}{1-d_S}.V_B$$

Since V_B is greater than V_S, d_B will always be lesser than d_S. Therefore, by controlling d_B and d_S, power flow from battery and supercapacitor to dc grid can be controlled independently.

2.2 HESS Charging Mode

When the generated power from photovoltaic (PV) sources surpasses the load demand or when the load diminishes, surplus power accumulates in the DC microgrid, leading to an elevation in the DC microgrid voltage. This excess power is then utilized to charge both the battery and supercapacitor. Consequently, in this operational mode, power flows from the DC microgrid to the Hybrid Energy Storage System (HESS).

The operation of the converter in this mode can be segmented into three distinct time intervals, as illustrated in Fig. 2. Switch pairs S_1 and S_6 are concurrently activated, while switch pairs S_2 and S_5 receive complementary pulses relative to S_1 and S_6. Similarly, switches S_4 and S_3 are also activated in a complementary manner. At the initial time, t_0, switches S_1, S_4, and S_6 are turned on to linearly increase the inductor currents, i_B and i_S, in the negative direction with slopes V_{DC}/L_B and V_{DC}/L_S, respectively. Inductors L_B and L_S store energy during this interval until time t_1. At t_1, switch pair S_1/S_6 is turned off, and to sustain inductor current i_S, the body diodes of switches S_2 and S_5 are activated.

The energy stored in inductor L_S is then used to charge the supercapacitor, while inductor current i_B freewheels through the body diode of switch S_2. Following the dead time interval for switch pairs S_1/S_6 and S_2/S_5, gating pulses are applied to S_2 and S_5, turning them on with zero voltage switching (ZVS) since the body diodes of

the respective switches are already conducting. At time t_2, switch S_4 is turned off, and inductor current i_S increases linearly with slope V_S/L_S through the body diode of switch S_3. After the dead time interval of switch pair S_4/S_3, a gating pulse is applied to S_3 to turn it on with ZVS. The energy stored in inductor L_B is now used to charge the battery. At time t_3, switches S_2, S_3, and S_5 are turned off, and as a result, the body diodes of switches S_1, S4, and S_6 turn on to maintain the flow of inductor currents. Gating pulses are then applied to S1, S_4, and S_6 after the dead time interval to turn them on with ZVS. If d_S is the duty cycle of the gating pulse for switch pair S_1/S_6, and d_B is the duty cycle of the gating pulse for switch S_4, applying the volt-second balance to inductors L_S and L_B yields.

$$V_S = \frac{d_S}{1-d_S}.V_{DC}$$

$$V_B = \frac{d_S}{1-d_B}.V_{DC}$$

2.3 HESS Energy Exchange Mode

The supercapacitor within the Hybrid Energy Storage System (HESS) serves as a unit with high power density. However, it lacks the capability to provide energy continuously for extended durations, as it experiences a substantial self-discharging effect. In the context of dc microgrid applications, it is imperative for the energy storage components (ESSs) of HESS to maintain sufficient stored energy for optimal operation.

To ensure the effective functioning of HESS, it becomes essential to charge the supercapacitor from the energy-dense battery whenever necessary. This operational mode involves the flow of power from the battery to the supercapacitor. The corresponding circuit topology for this mode is depicted in Figure 2.

In this operational mode, the first switch leg remains inactive, with switches S_1 and S_2 turned off, effectively isolating the dc microgrid from the Hybrid Energy Storage System (HESS) during the charging process of the supercapacitor. Switch pairs S_5/S_6 and S_3/S_4 operate in a complementary manner. Switch S_5 remains in the on state throughout this mode, resulting in switch S_6 being consistently off. Switch S_3 is modulated with a duty cycle denoted as d, and the corresponding waveforms are illustrated in Figure 2. The power flow from the battery to the supercapacitor involves the buck operation of switch S_3. Inductors L_B and L_S are connected in series, significantly reducing current ripple. By controlling the duty cycle, d, the power flow from the battery to the supercapacitor can be regulated. Applying a volt-second balance to the equivalent series inductor L (where $L = L_B + L_S$) yields.

$$V_S = d.V_B$$

2.4 Mode Transitions

The operational mode is determined based on the current state of the dc microgrid and continuous monitoring of the State of Charge (SOC) of the supercapacitor. For the purposes of this study, the State of Charge of the battery is not considered, as it is assumed that the battery's energy depletion rate is comparatively slow compared to that of the supercapacitor.

If the dc microgrid voltage surpasses the predefined reference value and the supercapacitor SOC is within the specified limits, the Hybrid Energy Storage System (HESS) is switched to charging mode. Conversely, when the dc microgrid voltage falls below the set reference value, and the supercapacitor SOC is within safe limits, HESS transitions to discharging mode. In cases where the supercapacitor SOC exceeds or violates the prescribed limits, HESS shifts to an energy exchange mode, effectively electrically isolating the dc microgrid from the HESS.

III. HESS CONTROL SCHEME

The control block diagrams for both the suggested and conventional control techniques are depicted in Figures 3 and 4, respectively. In both systems, a comparison is made between the grid's reference voltage ($V_{DC,ref}$) and the actual voltage (V_{DC}). The difference between these two voltages is then input into the Proportional-Integral (PI) scheduler. The processor receives the necessary total reference current (i_{tot}) from the Hybrid Energy Storage System (HESS), aiming to minimize voltage variations. In the conventional method illustrated in Figure 3, the overall current is divided into low and high-frequency components, which are then assigned as the respective reference currents for the battery and the supercapacitor (SC). Conversely, in the proposed control method, elaborated upon below, the battery current includes an error component, while the SC reference current comprises a high-frequency component.

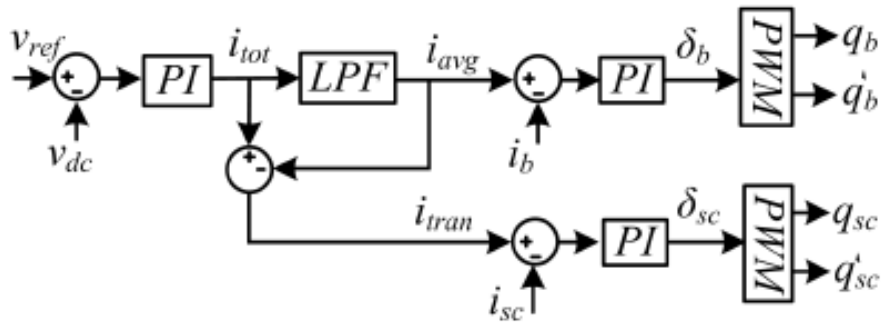

Figure 3 Conventional Control Scheme

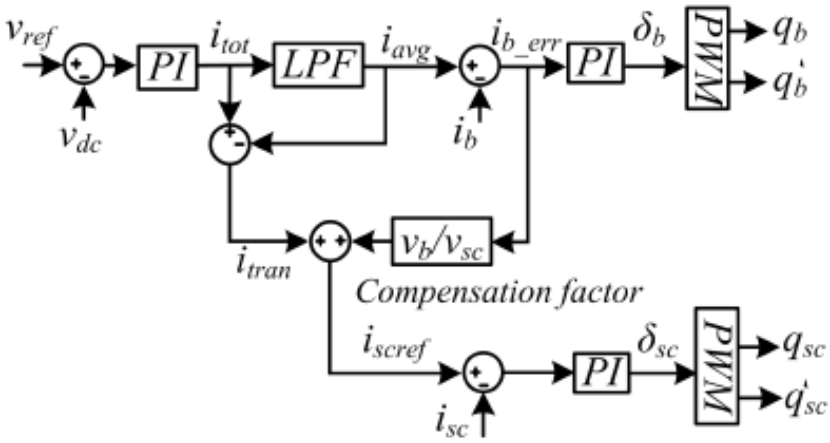

Figure 4 Proposed Control Scheme

3.1 Conventional Control Scheme

The schematic representation of the conventional control method employed for Hybrid Energy Storage System (HESS) control is presented in Figure 3. This conventional control method utilizes a dual-loop voltage control technique to manage the DC link voltage, comprising an inner control loop and an outer control loop. The inner control loop regulates the current from the HESS, while the outer control loop determines the current reference for the current control loop. The total current reference is generated to balance the overall power flow in the DC link during load and generation variations.

In the conventional method depicted in Figure 3, the DC link voltage (v_{dc}) is compared with the DC link voltage reference value (v_{ref}). The resultant error voltage is fed into the voltage control loop. The voltage loop Proportional-Integral (PI) compensator produces the total current reference (i_{tot}) to be supplied/absorbed by the HESS. itot is then divided into average current demand and transient current demand using a Low-Pass Filter (LPF), as illustrated in Figure 3. The average current (i_{avg}) and transient current (i_{tran}) serve as current references for the battery and supercapacitor (SC), respectively. It's important to note that the controller bandwidth of the voltage and current PI compensator must be judiciously selected to prevent conflicts within the converter controller. Furthermore, these controllers are designed to operate at specific operating points, and their

performance may degrade if the operating points change. Notably, the conventional control method tends to overlook the battery error current generated by the battery controller and the slow dynamics of the battery.

3.2 Proposed Control Scheme

The integrated control strategy addresses the aforementioned issues encountered in the conventional control method. The primary objectives of the proposed control strategy are to (i) improve battery lifetime, (ii) enhance DC link voltage regulation, and (iii) reduce stress on the battery system. The representation of the joint control strategy is depicted in Figure 3.5(b). This strategy is applied for controlling Hybrid Energy Storage Systems (HESS) with a Photovoltaic (PV) system in standalone DC microgrid applications. Similar to conventional control methods, the power required to balance the overall power flow in the DC link during load and generation variations is categorized into two components: (i) average power component (Pavg), and (ii) transient power component (Ptran).

The component (i_{lfc}) with low frequency is derived from i_{tot} as derived as follows,

$$i_{lfc} = f_{lfc}(i_{tot})$$

Where, low pass filter function is represented as $f_{lfc}(.)$. A rate limiter (f_{rl}) is introduced for battery current charge/discharge rate limit which is depicted in Figure 3. The current signal reference of rate limiter output is formulated by,

$$i_{BAT,ref} = f_{rl}(i_{lfc})$$

The difference in currents ($i_{BAT,err}$) is given to the PI controller after the battery current with reference and actual are contrasted with each other. The controller generates the control signal (d_B) to minimize the dissimilarity in the currents. The pulse width modulated (PWM) pulses are generated to the switches (S_{b1}, S_{b2}) in the converter of battery to the PWM generator, this duty ratio which is shown in Figure 3. In DC-DC converter due to the electrical inertia and slow dynamics of battery system the converter may not follow instantly with battery reference current ($i_{BAT,ref}$). Therefore, the uncompensated power is observed in battery system is given by

$$i_{tran} = i_{tot} - i_{BAT,ref}$$

$$P_{B\_Uncomp} = (i_{BAT,ref} - i_{BAT}) \cdot V_B$$

Where i_{tran}: transient component of current, P_{B_Uncomp}: battery uncompensated power. In the proposed control strategy P_{B_Uncomp} used to enhance the performance of SC. Therefore, the supercapacitor reference current ($i_{SC,ref}$) is formulated as follows,

$$i_{SC,ref} = i_{tran} + (i_{BAT,ref} - i_{BAT})\frac{V_B}{V_{SC}}$$

The error is passed to the controller after the actual and references of supercapacitor currents are contrasted with each other. The error is minimized when the PI controller generates the control signal d_{SC}. To generate the pulses of PWM corresponding to SC switches such as S_{c1}, S_{c2} this control signal is given to the PWM generator which is shown in Figure 3.

$$i_{SC,ref} = i_{tran} + i_{BAT,err} \cdot \frac{V_B}{V_{SC}}$$

Where $i_{BAT,err}$: battery error current is the difference between actual and references of battery is given by

$$i_{BAT,err} = i_{BAT,ref} - i_{BAT}$$

IV. SIMULATIONS RESULTS AND DISCUSSION

In this section, the outcomes of both the conventional and proposed control schemes are showcased. The nominal parameters utilized for the simulation study are outlined in Table 1. The entire model is implemented using MATLAB. The model comprises two bidirectional converters one dedicated to the battery and the other to the supercapacitor (SC). The Photovoltaic (PV) array is unidirectional, connected to the boost converter.

The following sections present the four operating cases, each involving a step change in PV generation and load demand.

4.1 Conventional Control Scheme

The simulation results for traditional control schemes are depicted in Fig 5, Fig 6, and Fig 7. Owing to atmospheric variations, the power generated by the Photovoltaic (PV) panel increases from 96W to 192W and then returns to 96W. Throughout this scenario, the load power requirement remains constant at 96W. Since the PV power exceeds the load power requirement, the DC grid voltage rises beyond 48V. To address this, the Supercapacitor (SC) promptly absorbs the excess power of 96W in a short duration, allowing the battery sufficient time to regulate the grid voltage back to 48V. Consequently, the battery and SC charge in accordance with the energy management strategy to sustain the DC grid voltage at a constant 48V.

Table 1 Rated parameters for simulation Analysis

S. NO	Speciicat ion	Value
1	Peak Power (Pmppt)	96 W
2	DC microgrid voltage (VDC)	48 V
3	Maximum Peak Power Current (Imppt)	4 A
4	Battery Voltage (VB)	24 V
5	Maximum Peak Power Voltage (Vmppt)	24 V
6	SC Voltage (VSC)	32 V
7	Resistanc e (R)	24 Ω
8	Battery inductance (LB)	0.4 mH
9	SC inductance (LS)	0.355 mH

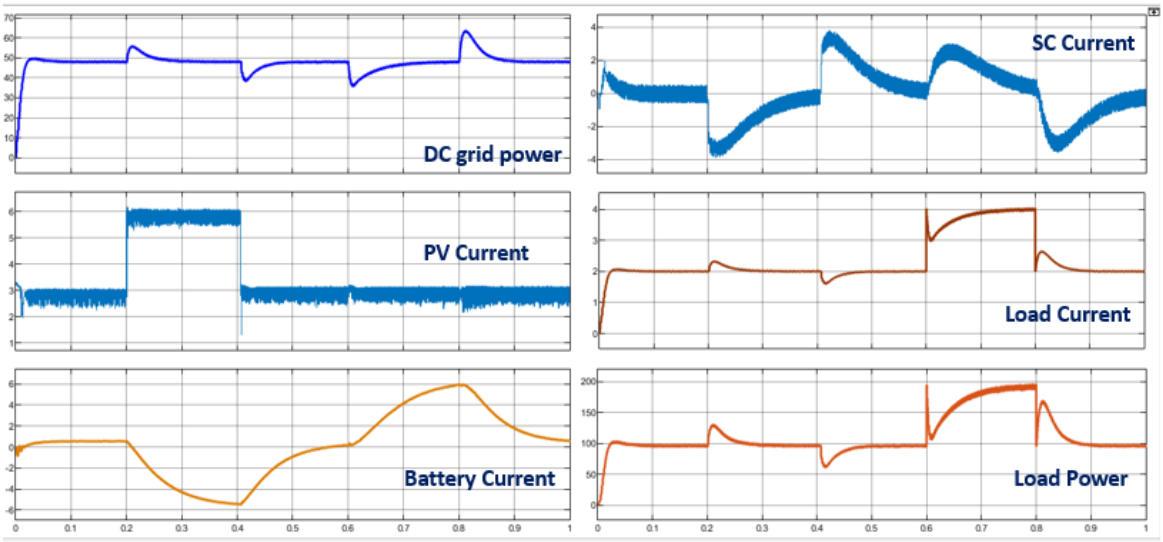

Fig 5 step change in conventional control scheme

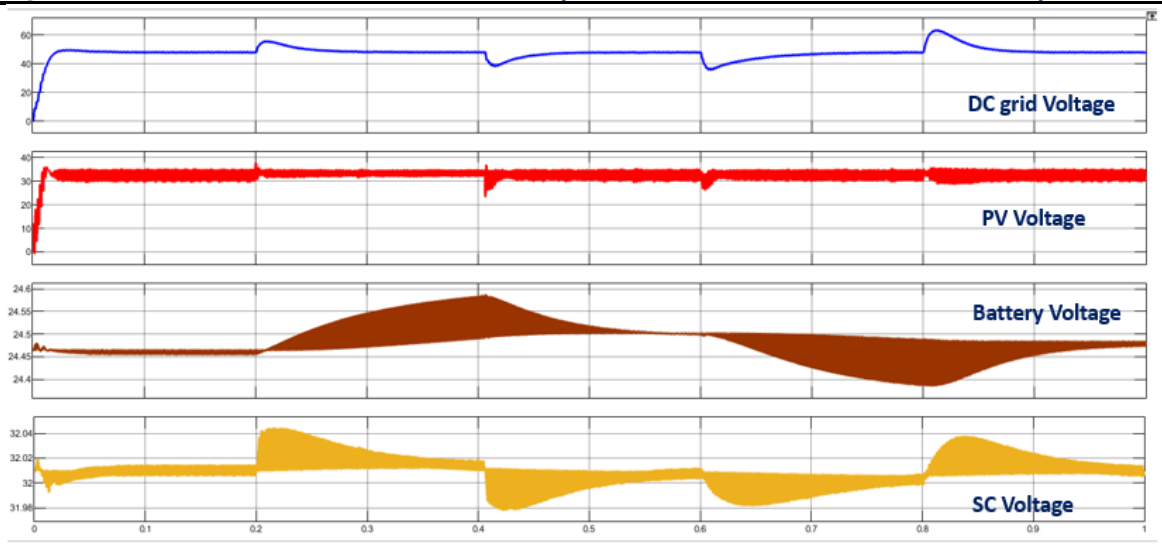

Fig 6 DC grid voltage change in conventional control scheme

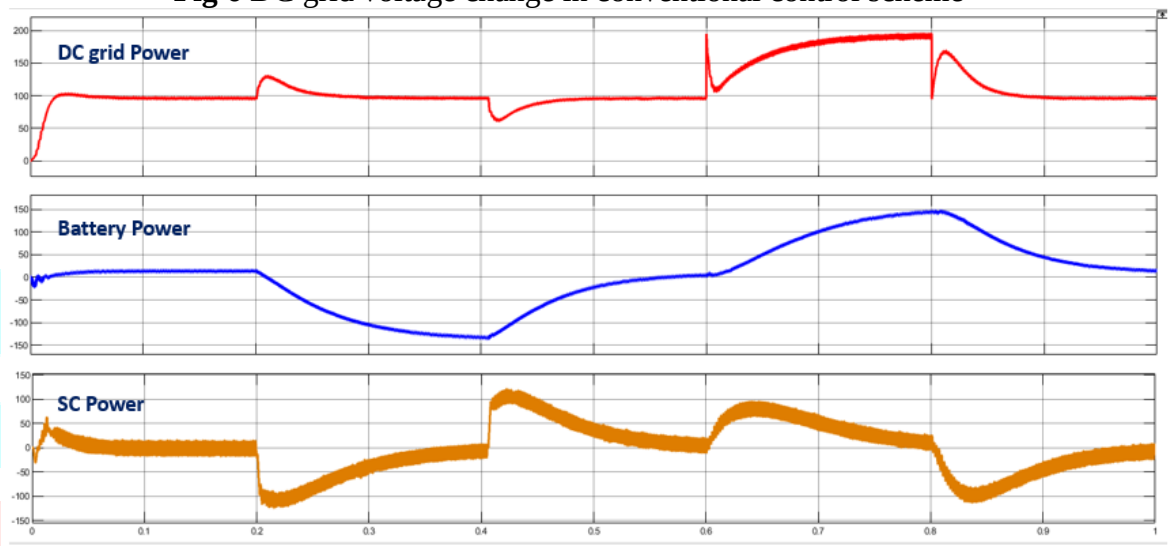

Fig 7 DC grid power change in conventional control scheme

4.2 Proposed Control Scheme

The simulation results for proposed control schemes are depicted in Fig 8 and Fig 9. Owing to atmospheric variations, the power generated by the Photovoltaic (PV) panel increases from 96W to 192W and then returns to 96W. Throughout this scenario, the load power requirement remains constant at 96W. Since the PV power exceeds the load power requirement, the DC grid voltage rises beyond 48V. To address this, the Supercapacitor (SC) promptly absorbs the excess power of 96W in a short duration, allowing the battery sufficient time to regulate the grid voltage back to 48V. Consequently, the battery and SC charge in accordance with the energy management strategy to sustain the DC grid voltage at a constant

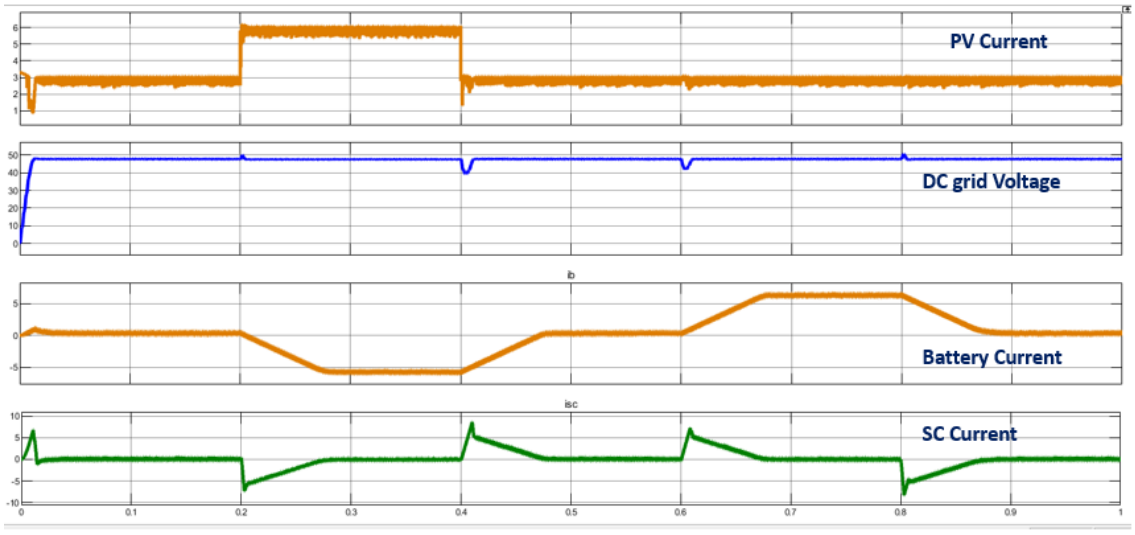

Fig 8 DC grid voltage change in proposed control scheme

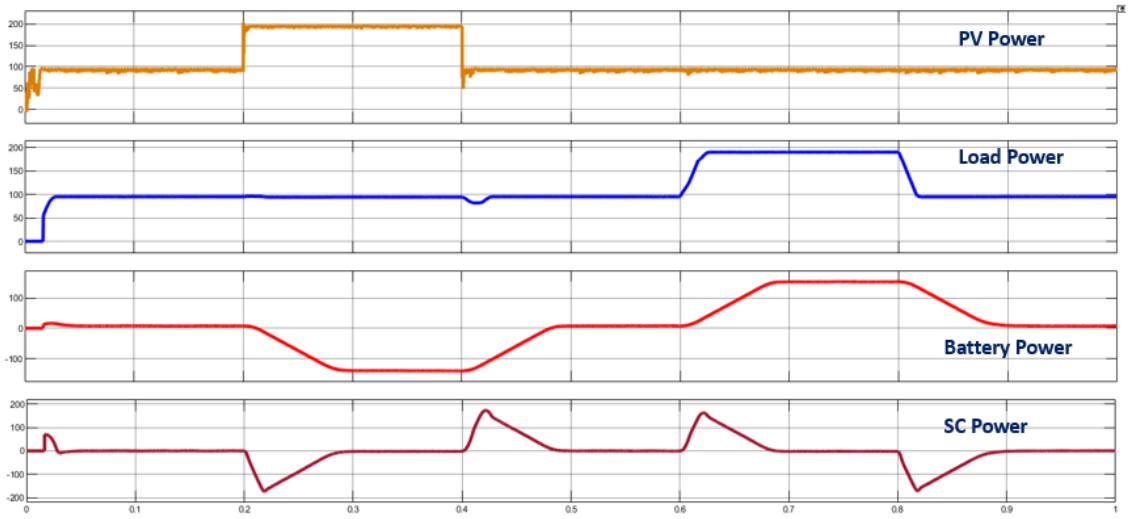

Fig 9 DC grid power change in proposed control scheme

4.3 Comparative Analysis

The performance of the proposed control scheme is evaluated in comparison to the conventional control scheme with step change in PV generation as well as load demand as shown in Fig 10, Fig 11 and Fig 12.

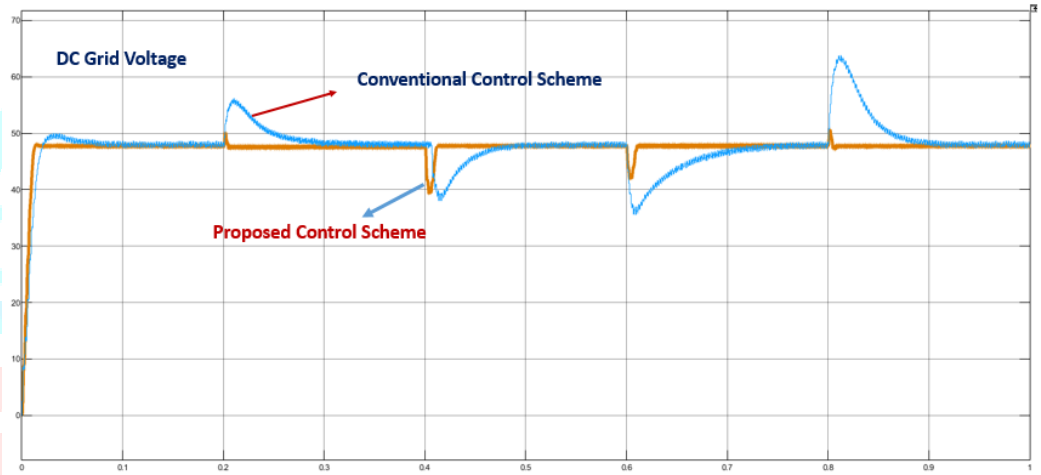

Fig 10 DC grid voltage change in Conventional vs proposed control scheme

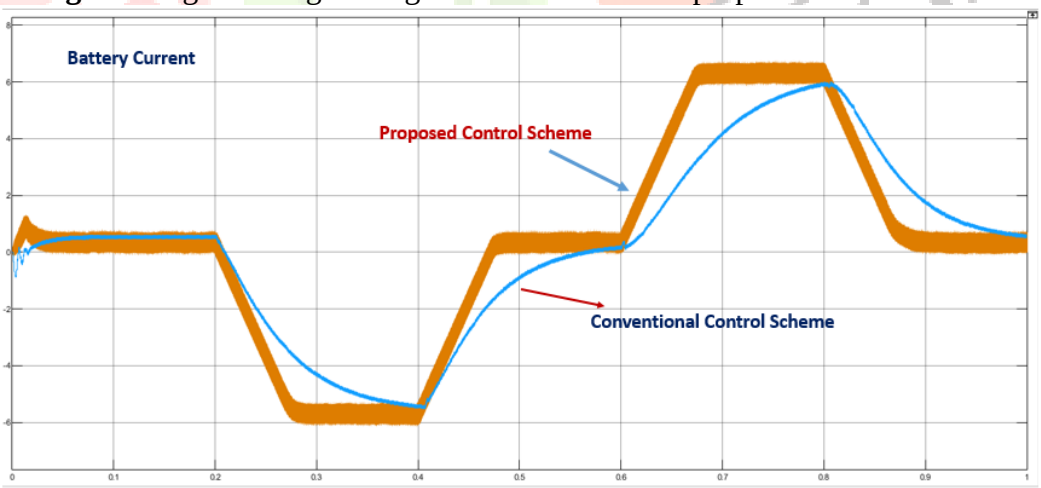

Fig 11 Battery current change in Conventional vs proposed control scheme

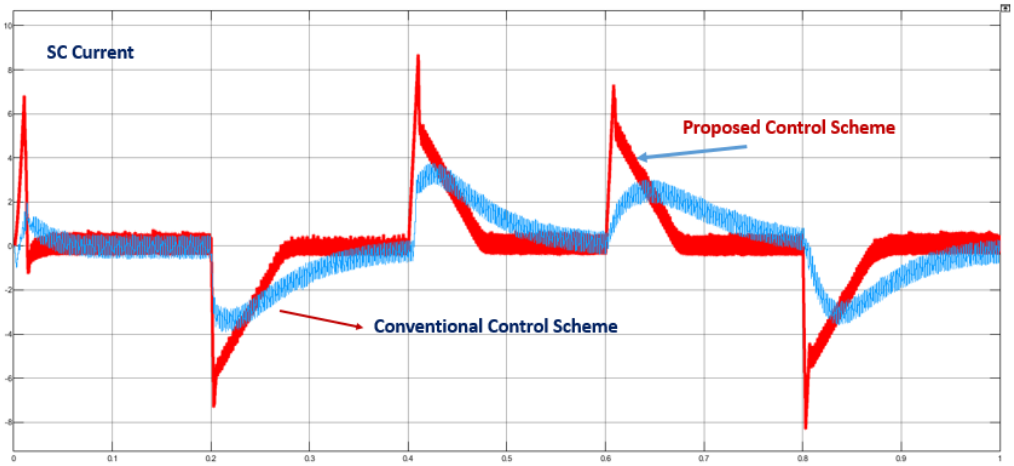

Fig 12 SC current change in Conventional vs proposed control scheme

V. CONCLUSION

A controller was devised for the bidirectional converter in the Hybrid Energy Storage System (HESS) to regulate its operation. The performance of the designed controller was evaluated under various scenarios with a focus on voltage regulation in the DC microgrid. The controller demonstrated effectiveness in stabilizing the DC microgrid against disturbances arising from both the source PV generation and load variations. Leveraging the inherent fast dynamics of the supercapacitor, the controller efficiently absorbed incoming transients to the microgrid. This unified controller proved capable of handling both the charging and discharging operations of the HESS. Furthermore, it achieved decoupled, separate, and independent control of supercapacitor and battery power, facilitating power flow between them. The versatility of this controller extends to applications such as hybrid electric vehicles, where two or more sources supply power. The operational mode of the HESS converter, ensuring the State of Charge (SOC) of the supercapacitor always remains within the desired limit, was also demonstrated.

REFERENCES

[1] Hredzak B., Agelidis V.G., Jang M. “A model predictive control system for a hybrid battery-ultracapacitor power source”. IEEE Transactions on Power Electronics, 2014. 29. Pp. 1469-1479.

[2] M. Glavin, P.Chan, S. Armstrong, W. Hurley, “A stand-alone Photovoltaic supercapacitor battery hybrid energy storage systems”, IEEE power electronics and Motion Control Conference, 2008, pp.1688-1695.

[3] M. Hamzeh, A. Ghazanfari, Y. A. I. Mohamed and Y. Karimi, "Modeling and Design of an Oscillatory Current-Sharing Control Strategy in DC Microgrids," in IEEE Transactions on Industrial Electronics, vol. 62, no. 11, pp. 6647-6657, Nov. 2015, doi: 10.1109/TIE.2015.2435703.

[4] G. Graditi, M. G. Ippolito, E. Telaretti and G. Zizzo, "An Innovative Conversion Device to the Grid Interface of Combined RES-Based Generators and Electric Storage Systems," in *IEEE Transactions on Industrial Electronics*, vol. 62, no. 4, pp. 2540-2550, April 2015.

[5] M.E Choi, S. W. Kim and S. W. Seo, "Energy Management Optimization in a Battery/Supercapacitor Hybrid Energy Storage System," in *IEEE Transactions on Smart Grid*, vol. 3, no. 1, pp. 463-472, March 2012.

[6] Punna, S.,Manthati, U.B, “Optimum design and analysis of a dynamic energy management scheme for HESS in renewable power generation applications”, *SN Appl. Sci.2*, 495, February 2020.

[7] O. Laldin,M. Moshirvaziri and O. Trescases,"Predictive Algorithm for Optimizing Power Flow in Hybrid Ultracapacitor/Battery Storage Systems for Light Electric Vehicles," in *IEEE Transactions on Power Electronics*, vol. 28, no. 8, pp. 3882-3895, Aug. 2013.

[8] Chia, Y.Y., Lee L.H., Shafiabady N., Isa D. “A load predictive energy management system for supercapacitor-battery hybrid energy storage system in solar application using the Support Vector Machine”. An International Journal of Applied Energy, 2015. 137. Pp. 588-602.

[9] Song Z., Hofmann H., Li J., Hou J., Han X., Ouyang M., “Energy management strategies comparison for electric vehicles with hybrid energy storage system”. An International Journal of Applied Energy, 2014. 134. Pp. 321-331.

[10] Torreglosa J.P., Garcia P., Fernandez L.M., Jurado F. “Predictive control for the energy management of a fuel-cell–battery–supercapacitor tramway”. IEEE Transactions on Industrial Informatics, 2014. 10. pp. 276-285.

[11] Bhomik P, Chandak S, Rout P K, State of Charge and State of Power Management in a Hybrid Energy Storage Systems by the Self-tuned Dynamic Exponent and the Fuzzy-Based Dynamic PI Controller. *Int Trans Electr Energ Syst*. 2019; e2848, doi; 10.1002/2050-7038.2848.

[12] C. Zhao, S.D Road and J.W. Kolar, " An Isolated Three-Port Bidirectional DC-DC Converter With Decoupled Power Flow Management," in *IEEE Transactions on Power Electronics*, vol.23,no.5,pp.2443-2453,Sept. 2008.

[13] J. Zeng, W. Qiao, L.Qu and Y. Jiao," An Isolated Multiport DC–DC Converter for Simultaneous Power Management of Multiple Different Renewable Energy Sources," in *IEEE Journal of Emerging and selected Topics an Power Electronics*, vol.2,no.1,pp.70-78,March 2014.

[14] Yifeng Wang, Fuqiang Han, Liang Yang, Rong xu, Ruixin liu, "A Three-Port Bidirectional Multi-Element Resonant Converter With Decoupled Power Flow Management for Hybrid Energy Storage Systems" *IEEE Access* volume 6, November 2018.

[15] P. Yang, C. K. Tse, J.Xu and G. Zhou, "Synthesis and Analysis of Double-Input Single-Output DC/DC Converter," in *IEEE Transaction on Industrial Electronics*, vol. 62, no.10,pp.6284-6295,Oct.2015.

[16] A. Khaligh, J. Cao and Y. J. Lee, "A Multiple-Input DC–DC Converter Topology," in *IEEE Transactions on Power Electronics*, vol. 24, no. 3, pp. 862-868, March 2009.

[17] Benfei Wang, Liang Xian, Ujjal Manandhar, Jian Ye, Xinan Zhang, Hoay Beng Gooi, Abhisek ukil, "Hybrid energy storage system using bidirectional single-inductor multipleport converter with model predictive control in DC microgrids" *Electric Power Systems Research*, 173 (April-2019),38-47.

[18] Rasoul Faraji, Hosein Farzanehfard," Soft-switching Nonisolated High step-up three-port DC-DC converter for Hybrid energy systems" *IEEE Transactions on Power Electronics*.vol.33, Dec-2018.

[19] Yusuke Sato, Masatoshi Uno, Hikaru Nagata, "Nonisolated Multiport Converters Based on Integration of PWM Converter and Phase-Shift-Switched Capacitor Converter" *IEEE Transactions on Power Electronics*, vol.35, no.1 January 2020.

[20] Zhehan Yi, Wanxin Dong, Amir H. Etemadi, "A Unified Control and Power Management Scheme for PV-Battery-Based Hybrid Microgrids for Both Grid-Connected and Islanded Modes," *IEEE Transactions on Smart grid*, vol.9, no.6, November 2018.

[21] H. Behjati and A. Davoudi," Power Budgeting Between Diversified Energy Sources and Loads Using a Multiple-Input Multiple-Output DC-DC Converter," in IEEE Transactions on Industry Applications,vol.49,no.6,pp. 2761-2772, Nov-Dec.2013.

[22] K.Filsoof and P. W. Lehn, " A Bidirectional Multiple-Input Multiple-Output Modular Multilevel DC-DC Converter and its Control Design," in IEEE Transactions on Power Electronics, vol.31,no.4,pp.2767-2779, April 2016.

[23] R. J. Wai, C. Y. Lin and B. H. Chen, "High-Efficiency DC-DC Converter With Two Input Power Sources," in IEEE Transactions on power Electronics,vol.27,no.4,pp.1862-1875,April 2012

[24] F. Nejabatkhah, S. Danyali, S.H. Hosseini, M. Sabahi and S. M. Niapour, "Modeling and Control of a New Three-Input DC–DC Boost Converter for Hybrid PV/FC/Battery Power System," in *IEEE Transactions on Power Electronics*, vol. 27, no. 5, pp. 2309-2324, May 2012.

[25] R. J. Wai B. H. Chen, "High-Efficiency Dual-Input Interleaved DC-DC Converter for Reversible Power Sources," in IEEE Transactions on Power Electronics, vol.29,no. 6,pp.2903-2921, June 2014.

[26] C. W. Chen, C. Y. Liao, K.H. Chen and Y. M. Chen, "Modeling and Controller Design of a Semiisolated Multiinput Converter for a Hybrid PV/Wind Power Charger System," in *IEEE Transactions on Power Electronics*, vol. 30, no. 9, pp. 4843-4853, Sept. 2015.

[27] S. Danyali, S. H. Hosseini and G. B. Gharehpetian, " New Extendable Single-Stage Multi-input DC–DC/AC Boost Converter," in *IEEE Transactions on Power Electronics*, vol. 29, no. 2, pp. 775-788, Feb. 2014.

[28] F. Guo, L. Fu, X. Zhang, C. Yao, H. Li and J. Wang, " A Family of Quasi-Switched-Capacitor Circuit-Based Dual-Input DC/DC Converters for Photovoltaic Systems Integrated With Battery Energy Storage," in *IEEE Transactions on Power Electronics*, vol. 31, no. 12, pp. 8237-8246, Dec. 2016.

[29] K. Gummi and M. Ferdowsi, " Double-Input DC-DC Power Electronic Converters for Electric-Drive Vehicles—Topology Exploration and Synthesis Using a Single-Pole Triple-Throw Switch," in *IEEE Transactions on Industrial Electronics*, vol. 57, no. 2, pp. 617-623,Feb.2010.

[30] R. R. Ahrabi, H. Ardi, M. Elmi and A. Ajami, "A Novel Step-Up Multiinput DC–DC Converter for Hybrid Electric Vehicles Application," in *IEEE Transactions on Power Electronics*, vol. 32, no. 5, pp. 3549-3561, May 2017.